The Astrophysical Journal, 832:128 (8pp), 2016 December 1 doi:10.3847/0004-637X/832/2/128

FLARE VERSUS SHOCK ACCELERATION OF HIGH-ENERGY PROTONS IN SOLAR ENERGETIC PARTICLE EVENTS

E. W. Cliver
National Solar Observatory, Boulder, CO, USA
Received 2016 March 30; revised 2016 June 15; accepted 2016 July 12; published 2016 November 22

ABSTRACT

Recent studies have presented evidence for a significant to dominant role for a flare-resident acceleration process for high-energy protons in large ("gradual") solar energetic particle (SEP) events, contrary to the more generally held view that such protons are primarily accelerated at shock waves driven by coronal mass ejections (CMEs). The new support for this flare-centric view is provided by correlations between the sizes of X-ray and/or microwave bursts and associated SEP events. For one such study that considered >100 MeV proton events, we present evidence based on CME speeds and widths, shock associations, and electron-to-proton ratios that indicates that events omitted from that investigation's analysis should have been included. Inclusion of these outlying events reverses the study's qualitative result and supports shock acceleration of >100 MeV protons. Examination of the ratios of 0.5 MeV electron intensities to >100 MeV proton intensities for the Grechnev et al. event sample provides additional support for shock acceleration of high-energy protons. Simply scaling up a classic "impulsive" SEP event to produce a large >100 MeV proton event implies the existence of prompt 0.5 MeV electron events that are approximately two orders of magnitude larger than are observed. While classic "impulsive" SEP events attributed to flares have high electron-to-proton ratios ($\gtrsim 5 \times 10^5$) due to a near absence of >100 MeV protons, large poorly connected (≥W120) gradual SEP events, attributed to widespread shock acceleration, have electron-to-proton ratios of $\sim 2 \times 10^3$, similar to those of comparably sized well-connected (W20–W90) SEP events.

Key words: Sun: coronal mass ejections (CMEs) – Sun: flares – Sun: particle emission

1. INTRODUCTION

The understanding of proton acceleration at the Sun in large solar energetic particle (SEP) events has oscillated between flare and shock pictures (Cliver 2009b; Reames 2015). The earliest picture following the discovery of ground-level events (GLEs; major SEP events requiring >500 MeV protons) by Forbush (1946) was that protons were accelerated in flares, the clear choice in the absence of other observations. Subsequently, Wild et al. (1963) conjectured, mainly on the basis of radio observations, that large SEP events required coronal shock waves as manifested by type II solar radio bursts. Smaller electron-dominated SEP events were linked to metric type III bursts. Early observational support for this view on the SEP side was provided by Lin (1970). Through the work of Švestka & Fritzová-Švestková (1974), Kahler et al. (1978, 1984), Cliver et al. (1982, 1983a, 1983b), Cane & Stone (1984), Klecker et al. (1984), Mason et al. (1984, 1986), Meyer (1985), Reames et al. (1985, 1994, 1996), Cane et al. (1986, 1988), Luhn et al. (1987), Reames (1990, 1999), Kahler (1992, 1994), Gosling (1993), and others, involving various comparisons of SEP events with flare electromagnetic emissions and coronal mass ejections (CMEs), as well as considerations of SEP composition, charge states, and the longitude distribution of SEP-associated flares, the two-class picture of SEP acceleration presciently proposed by Wild et al. (1963) became established. The new consensus view was almost immediately challenged by observations of the first large ("gradual"; Reames 1993) proton events observed by the *Advanced Composition Explorer* (*ACE*). Mazur et al. (1999), Cohen et al. (1999), Mason et al. (1999a), and Mason et al. (1999b) reported that large SEP events, including GLEs, recorded by *ACE* and SAMPEX in 1997 and 1998 had elemental composition and charge states at >10 MeV/nuc that were similar to those found in small ("impulsive") SEP events (e.g., Mason et al. 1986; Luhn et al. 1987) at lower energies. Subsequently, Cane et al. (2002, 2003, 2006) presented evidence based on low-frequency radio observations, SEP composition data, and flare location to argue for the presence of a flare-accelerated high-energy (>25 MeV) proton component in large SEP events to augment that produced by coronal/interplanetary shock waves driven by CMEs. The relative importance of flare and shock components was left as an open question.

The next key development in the field was the pioneering work by Tylka et al. (2005) that presented observational evidence and theoretical underpinning for the importance of shock geometry and seed particle populations for shock acceleration. They interpreted the 1997–1998 GLEs observed by *ACE* in terms of quasi-perpendicular shock acceleration of flare-accelerated seed particles. A related theoretical study by Tylka & Lee (2006) used their shock formulation to resolve the 20-year old puzzle presented by Breneman & Stone's (1985) finding that ionic charge-to-mass ratio (Q/M) "is the principal organizing factor for the fractionation of ...SEPs by acceleration and propagation processes and for flare-to-flare variability." This more-fully developed picture favoring a dominant role for shock acceleration in large SEP events—supported by correlations between CME speed and SEP intensity (Kahler 2001; Rouillard et al. 2012), studies considering shock seed particles (Kahler 2001; Cliver 2006), statistical studies on low-frequency radio bursts (Gopalswamy et al. 2002; Cliver et al. 2004), comparisons of electron and proton intensities in SEP events (Cliver & Ling 2007), considerations of flare and CME versus SEP energetics (Mewaldt et al. 2005; Gopalswamy et al. 2010; Emslie et al. 2012; Kahler & Vourlidas 2013), studies of SEP arrival time (Tylka et al. 2003; Reames 2009a, 2009b), analysis of SEP size distributions (Cliver et al. 2012), investigations of the temperature of SEP source regions

(Reames et al. 2015; Reames 2016), and a recent investigation of a widespread SEP event on 2014 February 25 observed by multiple spacecraft (Lario et al. 2016)—has found general acceptance (Reames 2013) over the alternative flare-based scenario. Studies of proton acceleration in large SEP events (e.g., Mewaldt et al. 2012; Desai et al. 2016) are increasingly framed in these terms. Nevertheless, a lively debate continues on the question of the principal source of high-energy protons in large SEP events. For example, Firoz et al. (2012) compared the timings of solar emissions with GLE onset times to attribute the 2005 January 20 GLE to a flare-resident SEP acceleration process.

Several recent papers (Dierckxsens et al. 2015; Grechnev et al. 2015; Trottet et al. 2015) have presented evidence for either a significant contributory (for 15–40 MeV protons, Trottet et al. 2015) or dominant (for >50 MeV protons, Dierckxsens et al. 2015; >100 MeV protons, Grechnev et al. 2015) role for a (unspecified) flare-resident particle acceleration mechanism (Miller et al. 1997; Drake et al. 2006; Cargill et al. 2012) in the generation of high-energy protons in large SEP events. The evidence for this view is based on the calculation of classical Pearson or partial correlation coefficients between the sizes (peak flux and or fluence) of X-ray and/or microwave bursts and associated SEP events. In this paper, we focus on the study of Grechnev et al. (2015) because, of the three studies, it considered the highest proton energy range. In Section 2, their correlation analysis between flare size (and also CME speed) and associated >100 MeV proton fluence is examined along with the 0.5 MeV electron intensity to >100 MeV proton intensity ratios of the events in their sample to gain insight on the relative importance of flares versus shocks for acceleration of high-energy particles at the Sun. Results are summarized and discussed in Section 3.

2. ANALYSIS

2.1. Correlation between >100 MeV Proton Fluence and 35 GHz Microwave Fluence

Figure 1 (adapted from Figure 6 of Grechnev et al. 2015) gives a plot of longitude-corrected >100 MeV fluence for proton events observed by the *Geostationary Operational Environmental Satellite* (*GOES*) monitors for the 1996–2014 time interval versus the 35 GHz radio fluence of the associated flares. Within the oval, $\log \Phi_{100}$ and $\log \Phi_{35}$ are highly correlated, with a partial correlation coefficient of 0.67, versus 0.001 for a corresponding comparison of $\log \Phi_{100}$ and log CME speed, leading Grechnev et al. (2015) to conclude that these SEP events originated in the associated flares. Partial correlation coefficients are designed to identify which of several possible parameters are most closely related to a given parameter, Φ_{100} in this case (for a detailed description of this technique see Trottet et al. 2015). In Figure 1, the events designated by squares for which the dates are indicated do not follow the trend of the events in the oval. In these cases, the >100 MeV fluence significantly exceeds that expected based on the size of the 35 GHz radio burst. Grechnev et al. (2015) suggest that these outlying, "abundant-proton," events originate in CME-driven shock waves. In Table 1, we compare the flare and SEP event parameters for the four well-connected (W21–W90; black circles) events in the orange rectangle in the oval (referred to as "main sequence" events) with the four outliers that have Φ_{100} values $>2 \times 10^5$ pfu s. Inspection of the flare

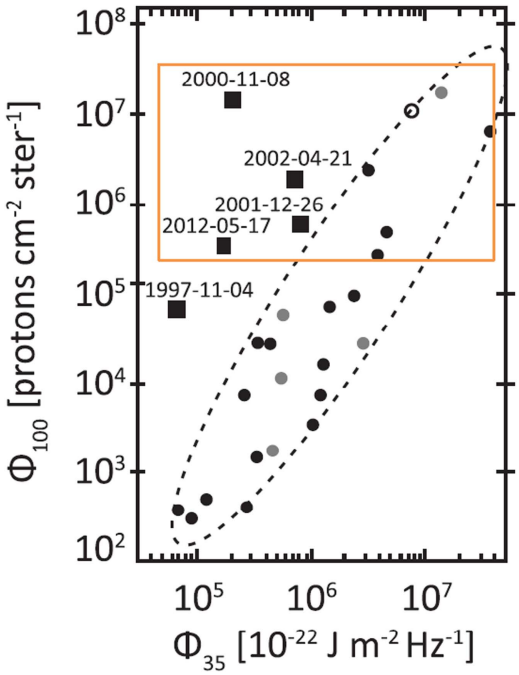

Figure 1. Scatterplot of longitude-corrected >100 MeV proton fluence (Φ_{100}) vs. 35 GHz fluence (Φ_{35}) for solar proton events from 1996 to 2014, adapted from Grechnev et al. (2015; black circles and squares (W21–W90); gray circles (E30–W20); open circles (<E30)). The orange rectangle isolates events with $\Phi_{100} > 2 \times 10^5$ pfu s.

parameters in Table 1 (taken from Grechnev et al. 2015) reveals that the four main sequence flare events are larger, with median value comparisons as follows: 1–8 Å soft X-ray (SXR) intensity classification (X5.8 for main sequence versus M7.8 for outliers), SXR fluence (405×10^{-3} J m^{-2} versus 88×10^{-3} J m^{-2}), and 35 GHz fluence (42×10^5 sfu s versus 4.6×10^5 sfu s). But this is also true for the associated CMEs: speed (2209 km s^{-1} versus 1660 km s^{-1}) and widths (360° versus >286°). Also, all of the main sequence events, as well as all of the outliers, have associated decametric/hectometric (DH; 1–14 MHz) type II bursts recorded by the Wind/Waves experiment (Bougeret et al. 1995). DH type II bursts are radio manifestations of strong coronal/interplanetary shocks and are highly associated with large SEP events (Gopalswamy et al. 2002; Cliver et al. 2004). Why would the DH type II shocks driven by the faster/wider CMEs in the main sequence events not also be strong accelerators of >100 MeV protons? Table 1 shows that the median Φ_{100} value for the main sequence events is 1.15×10^6 pfu s versus 1.05×10^6 pfu s for the outliers. The four main sequence and four outlier events were associated with three and two-to-three GLEs, respectively (see Thakur et al. 2016 for the 2000 November 8 outlier), with two of the main sequence GLEs being relatively large.

The last column in Table 1 gives the ratio of the peak hourly averaged 0.5 MeV (250–700 keV) electron intensity (recorded by the Comprehensive Suprathermal and Energetic Particle Analyzer (COSTEP; Müller-Mellin et al. 1995) on the *Solar and Heliospheric Observatory* (*SOHO*)) to the peak hourly averaged *GOES* >10 MeV proton intensity (above pre-event (or extrapolated pre-event) background for both species) for each event. Cliver & Ling (2007) showed that such ratios ranged from $\sim 2 \times 10^1$ to 4×10^2 for large shock-associated SEP events (their "population 2" or gradual events) versus

Table 1
Comparison of Large Outlying and Main Sequence SEP Events with >100 MeV Proton Fluence $>2 \times 10^5$ pfu s in Figure 6 of Grechnev et al. (2015)

	SXR	SXR	SXR	SXR	35 GHz	CME	CME	>100 MeV	GLE?/		0.5 MeV e- to 10
	SXR	SXR	SXR	SXR	35 GHz	CME	CME	>100 MeV	% Inc.	DH II?	0.5 MeV e- to 10 Mev pr
Date	Peak Time	Class	Duration	Fluence	Fluence	Speed	Width	Fluence			Ratio
Outliers	UT		minutes	10^{-3} J m^{-2}	10^5 sfu s (a)	km s^{-1}	°	10^3 pfu s(b)			
2000 Nov 8	23:27	M7.9	201	66	2.1	1738	>170	13000	yes?/-	yes	4.69E+01
2001 Dec 26	5:36	M7.6	306	110	8.2	1446	>212	600	yes/5	yes	8.44E+01
2002 Apr 21	1:47	X1.6	179	280	7.2	2393	360	1500	no/-	yes	7.13E+01
2012 May 17	1:47	M5.1	141	31	1.7	1582	360	305	yes/16	yes	5.20E+01
Main Sequence											
2001 Apr 2	21:51	X18.4	59	930	38	2505	244	220	no/ -	yes	1.12E+02
2002 Aug 24	1:11	X3.5	83	178	46	1913	360	400	yes/5	yes	1.62E+02
2005 Jan 20	7:00	X7.9	93	500	370	2800	360	6400	yes/269	yes	1.64E+02
2006 Dec 13	2:39	X3.7	82	310	32	1774	360	1900	yes/92	yes	1.78E+02

Note. (a) 1 sfu = 1 solar flux unit = 10^{-22} W m^{-2} Hz^{-1}; (b) 1 pfu = 1 proton flux unit = 1 pr cm^{-2} s^{-1} sr^{-1}. Data sources: http://www.ngdc.noaa.gov/stp/satellite/goes/dataaccess.html; http://cdaw.gsfc.nasa.gov/CME_list/; http://www-lep.gsfc.nasa.gov/waves/; http://cosmicrays.oulu.fi/GLE.html; http://www2.physik.uni-kiel.de/SOHO/phpeph/EPHIN.htm; Grechnev et al. (2015), Cliver & Ling (2009).

$\sim 2 \times 10^2$ to 4×10^4 for flare-associated ("population 1" or impulsive) events (for differential electron fluxes). For both groups of events in Table 1 the electron-to-proton ratio falls within the range for the gradual SEP events and falls well below that of the largest impulsive events. The slightly higher electron-to-proton ratios for the main sequence events may be a shock geometry effect, with the more impulsive flares on the main sequence (median full-width SXR duration at one-tenth of peak intensity = 82 minutes versus 190 minutes for the outliers) more likely to give rise to quasi-perpendicular shocks (Cliver 2009a, Gou & Giacalone 2010, Carley et al. 2013), which are thought to be efficient for electron acceleration.

In the partial correlation coefficient analysis of Grechnev et al. (2015; their Table 2), inclusion of the outliers in the sample decreases the correlation coefficient of 0.67 for a comparison of $\log \Phi_{100}$ with $\log \Phi_{35}$ to 0.09 and increases the coefficient from 0.001 to 0.33 for a comparison of $\log \Phi_{100}$ with log CME speed—reversing the qualitative result of the analysis, albeit with a smaller difference between the Φ_{35} (flare) and CME speed (shock) correlation coefficients.

2.2. Ratio of 0.5 MeV Electron Intensity to >100 MeV Proton Intensity

Table 2(a) gives solar flare, CME, shock, and SEP parameters for 22 well-connected (W21–W90) SEP events in Figure 1, including all of the outliers and 17 main sequence events. The longitude range of events is restricted to the zone of favorable Sun–Earth magnetic connection. Figure 2 contains a plot of the ratios of the peak hourly 0.5 MeV electron intensity to the peak hourly >100 MeV proton intensity (with both peak intensity values taken within 12 hr of SXR maximum in each case) versus the >100 MeV proton intensity for these events. The three red circles in the figure indicate the only three cases for which a DH type II burst was not observed. Thus they are good candidates to be "pure flare" events—a view that is supported by their weak proton emission and high electron-to-proton ratios (e.g., Lin 1970; Cliver & Ling 2007). Light blue circles indicate events that were associated with DH type II bursts and are presumed to be shock-dominated—an assumption that will be examined below.

If the flare process manifested by the three red circle points in Figure 2 were to give rise to large >100 MeV proton events, we would expect to see points, such as that indicated by the red square, with high electron-to-proton ratios as one moves to the right on the plot. The red square represents a hypothetical flare-produced SEP event with an electron-to-proton ratio of 2×10^5, comparable to those of the three red circle events, and a peak proton flux of 2×10^2 pfu. Such an event would have an electron event with a peak intensity of 4×10^7 (cm^2 s sr MeV)$^{-1}$. The only two events in the figure with peak proton fluxes $>2 \times 10^2$ pfu had peak electron fluxes approximately two orders of magnitude smaller than this value: 5.39×10^5 (cm^2 s sr MeV)$^{-1}$ for 2000 November 8 and 2.36×10^5 (cm^2 s sr MeV)$^{-1}$ for 2005 January 20 (Table 2(a)). Thus, the absence of actual red square events in Figure 2 provides indirect support that the bulk of the >100 MeV protons observed for the larger events in Figure 1 do not originate in a flare-resident SEP acceleration process. Adding a large shock event (with peak proton (electron) flux of 2×10^2 pfu (4×10^5 (cm^2 s sr MeV)$^{-1}$), to the red square event would only reduce its electron-to-proton ratio to $\sim 1 \times 10^5$.

Figure 2 indicates that the correlation observed between Φ_{100} and Φ_{35} for the main sequence in Figure 1 is partially due to a mixture of large shock-dominated and smaller flare-dominated SEP events. The same blend of flare and shock events will appear in the Φ_{100} versus CME speed correlation, where the flare-dominated events typically have CMEs with lower speeds (Reames et al. 2014). These CMEs, consisting of mass expelled along open field lines (Kahler et al. 2001), are different from the closed loop eruptions that drive shocks (Vršnak & Cliver 2008) in the large gradual SEP events.

To substantiate the result in Figure 2, we consider two additional groups of events in Figure 3. The first, for which solar and SEP parameters are given in Table 2(b) are the largest impulsive SEP events, based on COSTEP 0.5 MeV electron intensity in Table 1 of Cliver & Ling (2009). Each of these six

Table 2
Analyzed SEP Events

Event No.	Date	SXR Peak Time (UT)	SXR Class	SXR Duration (minutes)	CME Width (degrees)	CME Speed (km s^{-1})	DH Type II	>100 MeV pr Intensity (pfu)	0.5 MeV e- Intensity (cm^2 s sr MeV)$^{-1}$	e-/pr Ratio (b)
(a) W21–W90 Events (Grechnev et al. 2015) (a)										
1	1997 Nov 4	5:58	X2.1	15	360	785	yes	2.31E+00	1.43E+04	6.19E+03
2	1999 Dec 28	0:48	M4.8	13	82	672	no	1.52E-02	3.11E+03	*2.05E+05*
3	2000 Nov 8	23:27	M7.9	200	>170	1738	yes	3.35E+02	5.39E+05	1.61E+03
4	2001 Apr 2	21:51	X18.4	58	244	2505	yes	4.99E+00	7.39E+04	1.48E+04
5	2001 Dec 26	5:36	M7.6	305	>212	1446	yes	4.61E+01	6.11E+04	1.33E+03
6	2002 Feb 20	6:12	M5.6	17	360	952	no	2.35E-02	8.23E+03	*3.50E+05*
7	2002 Apr 21	1:47	X1.6	178	360	2393	yes	2.22E+01	1.49E+05	6.71E+03
8	2002 Aug 24	1:11	X3.5	82	360	1913	yes	2.81E+01	4.92E+04	1.75E+03
9	2003 May 28	0:27	X3.9	47	360	1366	yes	8.19E-02	3.81E+03	4.65E+04
10	2003 May 29	1:05	X1.2	34	360	1237	yes	2.60E-02	3.02E+03	1.16E+05
11	2003 May 31	2:24	X1.0	56	360	1835	yes	7.01E-01	2.95E+04	4.21E+04
12	2004 Oct 30	6:18	M4.4	12	360	422	yes	2.04E-02	8.61E+02	4.22E+04
13	2004 Nov 10	2:13	X2.7	30	360	3387	yes	1.63E+00	2.08E+04	1.28E+04
14	2005 Jan 20	7:00	X7.9	92	360	3242(c)	yes	4.89E+02	2.36E+05	4.83E+02
15	2006 Dec 13	2:39	X3.7	82	360	1774	yes	8.58E+01	1.14E+05	1.36E+03
16	2010 Jun 12	0:57	M2.0	15	119	486	yes	2.09E-02	1.21E+03	5.77E+04
17	2011 Aug 4	3:57	M9.3	45	360	1315	yes	1.63E+00	5.54E+03	3.40E+03
18	2011 Aug 9	8:05	X6.9	11	360	1610	yes	2.03E+00	8.12E+03	4.00E+03
19	2012 Jan 23	3:59	M8.7	181	360	2175	yes	2.17E+00	9.45E+04	4.37E+04
20	2012 May 17	1:47	M5.1	141	360	1582	yes	1.79E+01	1.02E+04	5.68E+02
21	2012 Jul 6	23:08	X1.1	34	360	1828	yes	2.29E-01	7.35E+03	3.20E+04
22	2013 Oct 28	2:03	X1.0	44	360	695	no (d)	2.14E-02	6.29E+03	*2.94E+05*
(b) Large Impulsive SEP Events (W20–W90) (Cliver & Ling 2009)										
1	2000 May 1	10:26	M1.2	23	54	1360	no	<1.00E-02	3.58E+03	*>3.58E+05*
2	2001 Apr 14	17:23	C4.6	(e)	113	830	no	<1.00E-02	3.61E+03	*>3.61E+05*
3	2002 Aug 18	21:24	M2.4	55	140	682	no	3.22E-02	1.73E+03	*5.37E+04*
4	2002 Aug 19	10:34	M2.2	29	102	549	no	1.22E-02	8.20E+03	*6.72E+05*
5	2002 Aug 19	21:02	M3.4	19	>66	712	no	1.06E-02	3.55E+03	*3.35E+05*
6	2002 Aug 20	8:26	M3.4	13	>122	1099	no	<1.00E-02	4.18E+04	*>4.18E+06*
(c) Large SEP Events from ⩾W120 (Cane et al. 2010; Richardson et al. 2014) (f)										
Event No.	Date	Type III Onset (UT)	…	…	CME Width (degrees)	CME Speed (km s^{-1})	DH Type II	>100 MeV pr Intensity (pfu)	0.5 MeV e- Intensity (cm^2 s sr MeV)$^{-1}$	e-/pr Ratio
1	1998 Nov 14	5:00	…	…	Data Gap	Data Gap	yes	5.40E+00	8.41E+04	1.56E+04
2	1999 Apr 24(g)	13:00	…	…	360	1495	yes	2.47E-02	9.30E+02	3.76E+04
3	1999 Jun 1(g)	18:45	…	…	360	1772	yes	4.23E-01	3.48E+03	8.22E+03
4	2001 Apr 18	2:20	…	…	360	2465	yes	1.19E+01	1.33E+04	1.12E+03
5	2001 May 7	~8:55	…	…	233	604	no	3.73E-02	4.05E+02 (h)	1.09E+04
6	2001 Jun 15	~15:30	…	…	360	1701	yes	1.99E-01	3.88E+03	1.95E+04
7	2001 Aug 15	~23:55	…	…	360	1575	yes	2.68E+01	9.71E+04	3.63E+03
8	2003 Nov 2	9:20	…	…	360	2036	yes	4.33E-02	1.99E+03	4.61E+04
9	2004 Nov 1	~6:00	…	…	146	925	yes	1.09E+00	7.60E+03	6.99E+03
10	2011 Mar 21	~02:15	…	…	360	1341	yes	1.45E-01	4.89E+02	3.37E+03
11	2012 Jul 23(g)	~02:00	…	…	360	2003	yes	6.24E-01	4.86E+03	7.79E+03
12	2013 Dec 28	~17:00	…	…	360	1118	no (d)	1.66E-01	3.80E+02	2.29E+03

Note. (a) We excluded a weak western hemisphere event on 2007 September 7 with a partial gap in the COSTEP electron record; (b) Values in italics indicate a front-side event that lacked a DH type II radio burst; these events are plotted with red symbols, denoting a flare event, in Figures 2 and 3. (c) Estimate from Gopalswamy et al. (2005); (d) DH type II identifications on the NASA Waves website are incomplete after 2012; for this event we determined the absence of an associated burst from the daily summary plots; (e) Impulsive event, but the SXR peak was less than a factor of 10 above background; (f) W120 is the largest western longitude indicated for any flare by Cane et al. (2010) and it represents a lower limit; (g) The peak prompt electron and/or proton intensity were taken from 13 to 18 hr after the peak of the associated SXR burst. (h) A later peak at 22 UT is attributed to a subsequent flare. Data sources: www.ngdc.noaa.gov/stp/satellite/goes/dataaccess.html; http://cdaw.gsfc.nasa.gov/CME_list/; http://www-lep.gsfc.nasa.gov/waves/; http://www2.physik.uni-kiel.de/SOHO/phpeph/EPHIN.htm.

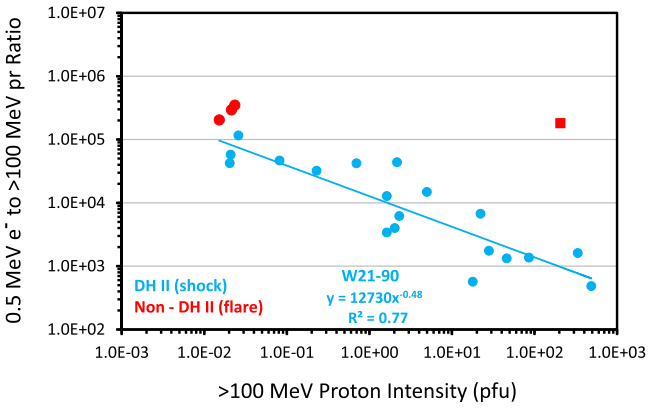

Figure 2. Electron-to-proton ratio vs. >100 MeV peak proton intensity for well-connected events in Figure 1. Red circles indicate events that lacked associated DH type II emission and are thus candidate flare-dominated events. Light blue circles indicate events that are presumed to be shock-dominated. The red square corresponds to a hypothetical large (2×10^2 pfu) "pure flare" SEP event.

events (taken from a compilation of large impulsive SEP events by Reames & Ng (2004) based on ^{3}He/^{4}He and Fe/O ratios and Fe intensity for the 1994 November to 2003 September time period) had peak electron intensities $>10^3$ (cm^2 s sr MeV)$^{-1}$ and all were located between W20–W89 (Nitta et al. 2006). None of these six events were associated with a DH type II radio burst (Cliver & Ling 2009). These events are indicated by either red triangles (for events with lower limit electron-to-proton ratios) or red diamonds in Figure 3. The median electron-to-proton ratio for the six events in Table 2(b) is $\gtrsim 4 \times 10^5$. The addition of these large flare-associated SEP events emphasizes the difference between the events with and without DH type II bursts, although there is overlap in the plot for the smaller events of either group. The difference between SEP events that arise in flares and those that we believe originate in coronal/interplanetary shocks is illustrated in Figure 4, which shows two examples of each, with flare events in (a) and (b) and shock events in (c) and (d). While the acceleration of 0.5 MeV electrons is comparable in all four cases, >100 MeV protons are absent or nearly so in the flare events.

The second group of SEP events that we add to Figure 3 is taken from the compilations by Cane et al. (2010) and Richardson et al. (2014). From their tables we selected the 12 large [$\geqslant$0.1 pr (cm^2 s sr Mev)$^{-1}$] 25–30 MeV proton events from 1997 to 2009 for which the authors identified a source nominally located at W120. (To avoid complex particle intensity time profiles due to the passage of shocks at Earth, we did not consider poorly connected events originating east of W21.) Solar and SEP parameters for these 12 events are given in Table 2(c). Because of their origins ~60° or more from the nominal ~W60 footpoint of the Parker spiral to Earth, such SEP events, designated by black squares in Figure 3, are presumed not to arise in flares (because of the limited SEP "cones of emission" for flares, e.g., Kallenrode et al. 1992) and are generally attributed to widespread SEP acceleration at CME-driven shock waves (e.g., Cliver 1982; Cliver et al. 2005; Kahler 2016). The data points for these events scatter about the light blue circle points of the Grechnev et al. (2015) front-side events for events with peak >100 MeV proton fluxes >1 pfu, but generally fall below the front-side data points for lower-intensity (<1 pfu) events.

The convergence of the red data points (flare-associated SEP events) with those of the light blue data points (shock-associated SEP events) for low intensity proton events in Figure 3 suggests that the light blue events represent a mixture of flare- and shock-accelerated SEP populations. To test this likelihood, we added a nominal large flare SEP event (with peak electron intensity of 3.6×10^3 (cm^2 s sr Mev)$^{-1}$ and peak proton intensity of 1×10^{-2} pfu, based on median values for the six events in Table 2(b)) to each of the 12 poorly connected presumed pure shock events. The result is shown in Figure 5. The power-law fit to the orange circle data points that represent the synthetic hybrid (pure flare plus pure shock) SEP events closely matches the fit through the well-connected Grechnev et al. (2015) events with DH type II association. This close match supports the conjecture that the light blue circle points represent blended events consisting of a flare and shock component. For events with a >100 MeV peak proton intensity below ~1 pfu, flare-accelerated electrons are primarily responsible for the increase in electron-to-proton ratio that brings the fit through the poorly connected black square events (in Figure 3) into agreement with that through the well-connected light blue circles. The effect of the 0.01 pfu flare proton contribution on the electron-to-proton ratios of the hybrid events is small to negligible across the peak >100 MeV proton intensity range of the poorly connected events.

This simple hybrid exercise supports the notion that the black square events are predominantly due to SEP acceleration by widespread shocks—a flare SEP component appears to be missing. The fact that the black square data points for the behind-the-limb events with peak >100 MeV proton fluxes >1 pfu overlap with the scatter of the light blue data points for comparably sized front-side events indicates that >100 MeV proton acceleration in large front-side SEP events is also dominated by shock acceleration. For SEP events with >100 MeV peak proton intensities >10 pfu, median electron-to-proton ratios for both back-side and front-side events are ~1–2 $\times 10^3$.

3. CONCLUSION

3.1. Summary

We considered recent studies (Dierckxsens et al. 2015; Grechnev et al. 2015; Trottet et al. 2015) that suggest that solar flares are significant sources of the high-energy protons observed in interplanetary space following solar eruptions and may, in fact, be the dominant accelerator of such protons. We used the Grechnev et al. (2015) study as our point of departure because, of the three studies, it considered the highest proton energy (>100 MeV). The evidence provided in all three studies was correlative, suggesting that the relationships between flare (SXR or radio emission) and proton event sizes were comparable to or stronger than those between CME speeds (indicative of shock acceleration) and SEP event fluxes or fluences.

In the Grechnev et al. (2015) study, correlative evidence for the acceleration of >100 MeV protons in a flare-resident process was found by omitting a subset of "abundant-proton" events with relatively weak flare emissions that were thus attributed to shock rather than flare processes (Figure 1). We argue that the exclusion of outlying events in the Grechnev et al. (2015) comparison of log >100 MeV proton fluence (Φ_{100}) and log 35 GHz radio fluence (Φ_{35}) is not warranted. A

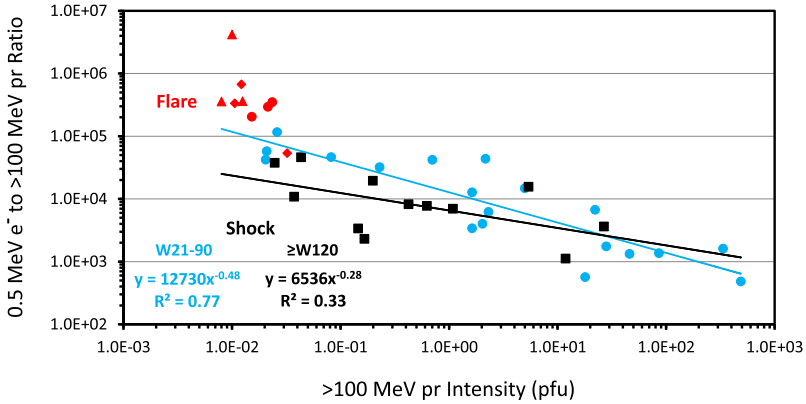

Figure 3. Electron-to-proton ratio vs. >100 MeV peak proton intensity for (a) W21–W90 events in Figure 1 (light blue and red circles with the red (light blue) events presumed to be due to flares (shocks); Grechnev et al. 2015); (b) W20–W89 flare-associated SEP events (red triangles (upper limits) and diamonds; Cliver & Ling 2009); and (c) large SEP events that originated at ⩾W120 (black squares; Cane et al. 2010 and Richardson et al. 2014). Two flare data points from (b) with coordinates of (<1.0E-2, >3.5E+05) were slightly offset in proton intensity for visibility.

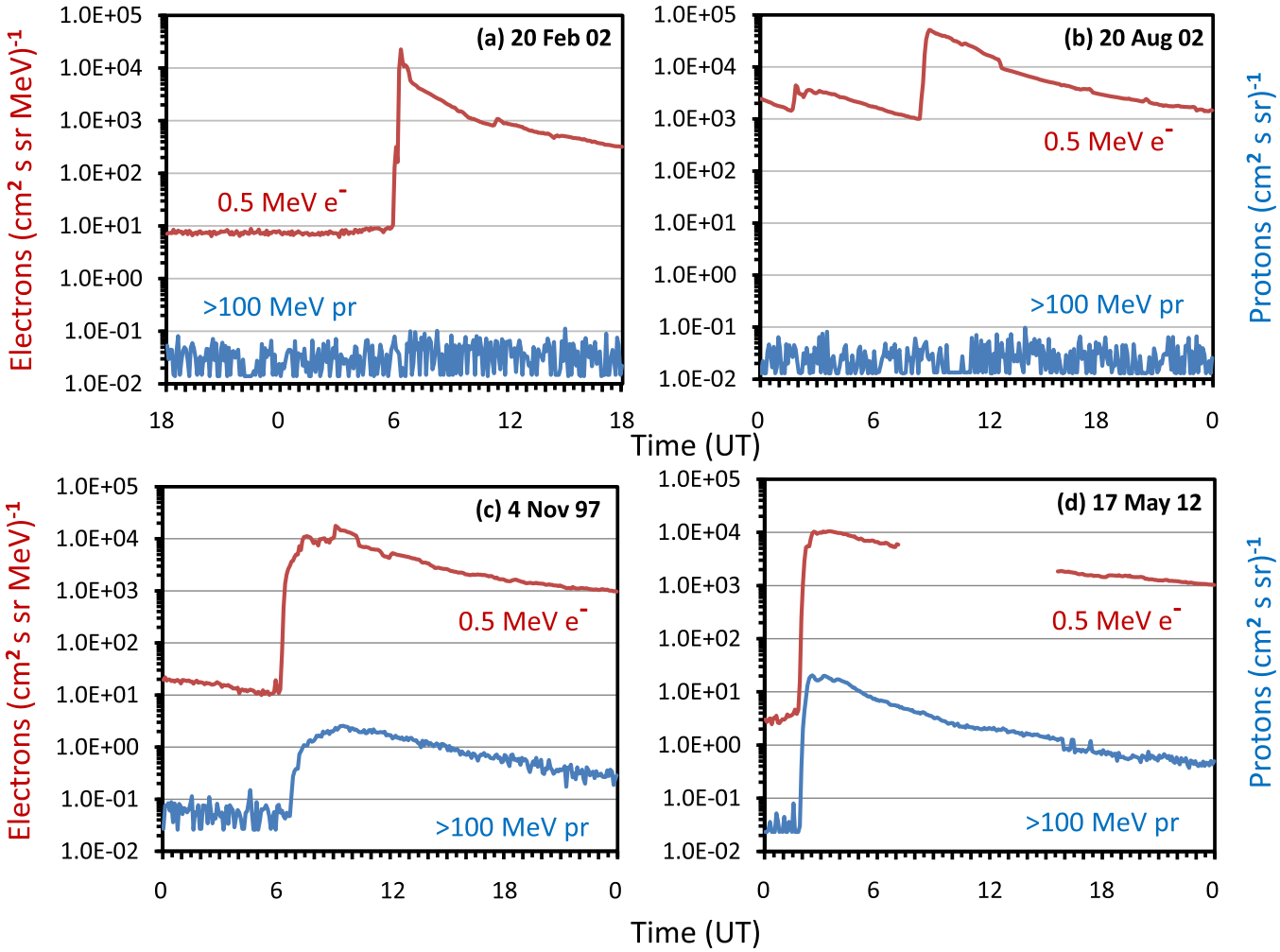

Figure 4. Comparison of 0.5 MeV electron and >100 MeV proton intensity time profiles in flare-associated (a, b) and shock-associated (c, d) SEP events.

comparison of CME speeds and widths, DH type II association, and SEP event electron-to-proton ratios for the excluded events with those of comparably sized SEP events on the main sequence of the scatter plot in Figure 1 revealed no significant differences between the two groups (Table 1). There is no compelling reason to expect that fast CMEs and their associated coronal/interplanetary shocks would be less efficient at accelerating high-energy protons in SEP events associated with strong flares events than they are at accelerating high-energy protons in the excluded events with weaker flare emissions. As documented in Table 2 of Grechnev et al. (2015), inclusion of these outlying events in the correlation

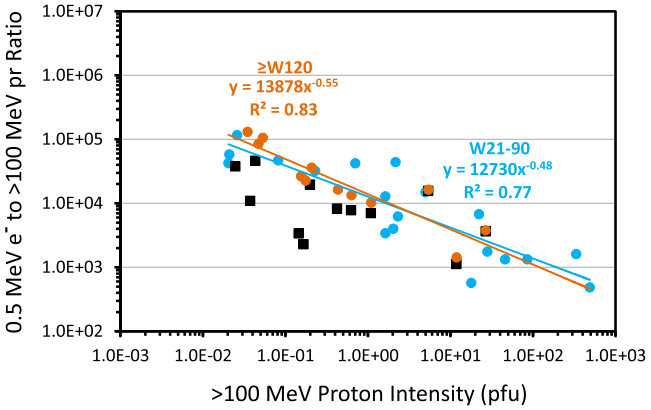

Figure 5. Electron-to-proton ratio vs. >100 MeV peak proton intensity for (a) W21–W90 events in Figure 1 (light blue circles; Grechnev et al. 2015); (b) large SEP events that originated at ⩾W120 (black squares; Cane et al. 2010 and Richardson et al. 2014); and (c) events in (b) to which a nominal large impulsive SEP event has been added (orange circles).

analysis reduces the partial correlation coefficient between $\log \Phi_{100}$ and $\log \Phi_{35}$ from 0.67 to 0.09, while increasing that between $\log \Phi_{100}$ and log CME speed from 0.001 to 0.33.

We examined the ratios of 0.5 MeV electron to >100 MeV proton intensities for the 22 well-connected (W21–W90) SEP events in Figure 1 (Grechnev et al. 2015), making comparisons with the corresponding ratios for a sample of 6 well-connected (W20–W89) large impulsive (flare-attributed) SEP events, and 12 events that originated at longitudes ⩾120° of solar central meridian (and are therefore presumably shock-dominated), and obtained the following results:

(a) Scaling up a classic flare-resident SEP event (e.g., the large impulsive events in Table 1 of Reames & Ng 2004) to produce a large >100 MeV proton peak intensity implies 0.5 MeV electron peak intensities approximately two orders of magnitude above any yet observed (e.g., Cliver & Ling 2007, 2009) during a prompt SEP event. We conclude that the flare-resident acceleration process is a poor producer of >100 MeV protons in SEP events (Figures 2–4).

(b) In Figure 3, large (>1 pfu) well-connected (W21–W90) and poorly connected (⩾W120) >100 MeV proton events have similar electron-to-proton ratios. In Figure 5, a simple exercise indicates that such large ⩾W120 proton events lack a flare component and originate in widespread shocks, as expected. Thus, we infer that in large well-connected SEP events—where acceleration of >100 MeV protons by a flare-resident acceleration process might be expected to play an important role—high-energy proton acceleration is dominated by CME-driven shocks.

3.2. Discussion

Figure 1 is reminiscent of Figure 2 in Cliver et al. (1989), which is a scatterplot comparing the peak fluxes of ∼10 MeV protons for SEP events from 1980 February to 1985 January with the prompt 4–8 MeV gamma-ray-line (GRL) fluences from the associated flares. Like Figure 1, the ∼10 MeV flux versus GRL fluence plot also shows a main sequence and outlying events, specifically, large proton events on 1981 July 20 and 1981 December 9 that lacked detectable GRL emission. These are early examples of the "proton-abundant" events of Grechnev et al. (2015), i.e., large proton events without commensurate flare emission. Cliver et al. (1983b) drew attention to such large prompt proton events following flares with "weak impulsive phases," and like Grechnev et al. (2015), attributed them to shock acceleration. Unlike Grechnev et al., however, the observation of strong SEP production in the absence of classic "big flares" led Cliver et al. to question the necessity of prominent big flares, such as those on the "main sequence" in Figure 1, for the acceleration of the energetic solar protons observed in space. They reasoned that if strong flares were not required for significant proton acceleration in the SEP events associated with "weak impulsive phase" flares, they might also be extraneous for SEP events following classic big flares and argued that the elements that were observed or inferred for the proton events following over-achieving "proton-abundant" flares—viz., mass ejection and shock formation—were the essential elements for significant proton acceleration at the Sun. The large proton events considered by Cliver et al. (1983b) had peak >10 MeV fluxes of ⩾10 pfu. The largest event in their sample, a GLE on 1979 August 21, had a peak >10 MeV flux of 500 pfu (ftp://ftp.swpc.noaa.gov/pub/indices/SPE.txt; Cliver et al. 1983a).

The value of the recent studies by Trottet et al. (2015), Dierckxsens et al. (2015), and Grechnev et al. (2015) lies in their focus on higher-energy protons, because it is now generally accepted (e.g., Cane et al. 2003; Trottet et al. 2015) that shocks dominate proton acceleration at energies below ∼20 MeV in large SEP events. In Figure 1, we see that the outlying events are copious producers of >100 MeV protons. The 2000 November 8 SEP event had the second highest peak >100 MeV intensity of any event in Figure 1. We know from gamma-ray observations that protons with energies >100 MeV can be rapidly generated in solar flares (Forrest & Chupp 1983). For example, pion-decay emission (requiring protons with a minimum energy of ∼300 MeV for pion production) was detected during the impulsive phase of the 1982 June 3 flare (Forrest et al. 1985; Chupp et al. 1987). The ensuing proton event observed at Helios (McDonald & Van Hollebeke 1985) on 1982 June 3, however, had an unusually hard spectrum that was more consistent with a second, extended, phase of pion-decay-dominated emission observed for this event. Ramaty et al. (1987) suggested that the SEP event at Helios was produced by proton acceleration at a coronal shock wave, with ∼4% of the shock-accelerated protons precipitating back to the Sun to produce late phase hard-spectrum gamma-ray emission (see Ryan & Lee 1991; Ryan 2000).

Reames (2015) touched on the point of a possible flare source of the high-energy protons observed in space in a recent review paper, writing, "If one were to invoke a flare component for large SEP events like GLEs, then that acceleration mechanism would have to differ from the one for acceleration of ^{3}He or Fe-rich events. It would also be one that no one has been able to characterize, one that hides under the cover of the dominant shock acceleration without altering its spectra." From the work done here, we agree, based on the examination of electron-to-proton ratios in Figures 2–5, that any such flare-resident particle acceleration process capable of producing large numbers of high-energy protons would have to differ from that producing classic ^{3}He or Fe-rich impulsive SEP events such as those in Table 2(b). Moreover, if the large main sequence >100 MeV protons in Figure 1 are accelerated in

solar flares rather than at shocks, one would need to explain a host of other observations consistent with the prevailing shock picture for large SEP events (see introduction), e.g., the observation of a prompt SEP event at widespread locations in conjunction with the longitudinal propagation of a white-light shock (Lario et al. 2016), in terms of such a flare-resident SEP acceleration mechanism. The possibility of a "hidden" flare source of protons observed in space with energies >100 MeV calls for further comparisons of flare high-energy gamma-ray emission, observed either in the impulsive phase or during an extended phase (Ackermann et al. 2012; Ajello et al. 2014; Pesce-Rollins et al. 2015), and associated SEPs.

There is another more recent observation that raises the possibility of a flare source for high-energy SEPs. McCracken et al. (2012) reported that certain GLEs (10 of 71 observed to date), which they termed "high-energy impulsive GLEs" or HEIGLEs, began with an impulsive rise (3–5 minutes) and rapid fall (dropping by 50%–70% from the peak within another 3–5 minutes) phase. Protons in HEIGLEs can reach energies up to 10–30 GeV. While the timescales of HEIGLEs are suggestive of a flare timescale (e.g., Drake et al. 2006), McCracken et al. (2012) noted that a quasi-perpendicular shock sweeping past the footpoint of the spiral field line to Earth might also account for the rapid "switch-on/switch-off" observed time profiles of HEIGLEs.

I thank Gerry Share for helpful input on recent gamma-ray work.

REFERENCES

Ackermann, M., Ajello, M., Allafort, A., et al. 2012, ApJ, 745, 144
Ajello, M., Albert, A., Allafort, A., et al. 2014, ApJ, 789, 20
Bougeret, J.-L., Kaiser, M. L., Kellogg, P.J., et al. 1995, SSRv, 71, 231
Breneman, H. H., & Stone, E. C. 1985, ApJL, 299, L57
Cane, H. V., Erickson, W. C., & Prestage, N. P. 2002, JGR, 107, 1315
Cane, H. V., McGuire, R. E., & von Rosenvinge, T. T. 1986, ApJ, 301, 448
Cane, H. V., Mewaldt, R. A., Cohen, C. M. S., & von Rosenvinge, T. T. 2006, JGR, 111, A06S90
Cane, H. V., Reames, D. V., & von Rosenvinge, T. T. 1988, JGR, 93, 9555
Cane, H. V., Richardson, I. G., & von Rosenvinge, T. T. 2010, JGR, 115, A08101
Cane, H. V., & Stone, R. G. 1984, ApJ, 282, 339
Cane, H. V., von Rosenvinge, T. T., Cohen, C. M. S., & Mewaldt, R. A. 2003, GeoRL, 30, 8017
Cargill, P. J., Vlahos, L., Baumann, G., Drake, J. F., & Nordlund, Å 2012, SSRv, 173, 223
Carley, E. P., Long, D. M., Byrne, J. P., et al. 2013, NatPh, 9, 811
Chupp, E. L., Debrunner, H., Flueckiger, E., et al. 1987, ApJ, 318, 913
Cliver, E. W. 2006, ApJ, 639, 1206
Cliver, E. W. 2009a, CEAB, 33, 253
Cliver, E. W. 2009b, in IAU Symp. 257, Universal Heliospheric Processes, ed. N. Gopalswamy & D. F. Webb (Cambridge: Cambridge Univ. Press), 401
Cliver, E. W., Forrest, D. J., Cane, H. V., et al. 1989, ApJ, 343, 953
Cliver, E. W., Kahler, S. W., Cane, H. V., et al. 1983a, SoPh, 89, 181
Cliver, E. W., Kahler, S. W., & McIntosh, P. S. 1983b, ApJ, 264, 699
Cliver, E. W., Kahler, S. W., & Reames, D. V. 2004, ApJ, 605, 902
Cliver, E. W., Kahler, S. W., Shea, M. A., & Smart, D. F. 1982, ApJ, 260, 362
Cliver, E. W., & Ling, A. G. 2007, ApJ, 658, 1349
Cliver, E. W., & Ling, A. G. 2009, ApJ, 690, 598
Cliver, E. W., Ling, A. G., Belov, A., & Yashiro, S. 2012, ApJL, 756, L29
Cliver, E. W., Thompson, B. J., Lawrence, G. R., et al. 2005, in Proc. 29th ICRC, ed. S. Acharya (Mumbai: TIFR), 1, 121
Cohen, C. M. S., Mewaldt, R. A., Leske, R. A., et al. 1999, GeoRL, 26, 2697
Desai, M. I., Mason, G. M., Dayeh, M. A., et al. 2016, ApJ, 816, 68
Dierckxsens, M., Tziotziou, K., & Dalla, S. 2015, SoPh, 290, 841
Drake, J. F., Swisdak, M., Che, H., & Shay, M. A. 2006, Natur, 443, 553
Emslie, A. G., Dennis, B. R., Shih, A. Y., et al. 2012, ApJ, 759, 71
Firoz, K. A., Gan, W. Q., Moon, Y.-J., & LI, C. 2012, ApJ, 758, 119
Forbush, S. E. 1946, PhRv, 70, 771
Forrest, D. J., & Chupp, E. L. 1983, Natur, 305, 291
Forrest, D. J., Vestrand, W. T., Chupp, E. L., et al. 1985, in Proc. ICRC, ed. F. C. Jones et al. (Washington, DC: NASA), 4, 146
Gopalswamy, N. 2010, in Heliophysical Processes, ed. N. Gopalswamy, S. Hasan, & A. Ambastha (Berlin: Springer), 53
Gopalswamy, N., Xie, H., Yashiro, S., & Usoskin, I. 2005, in Proc. 29th ICRC, ed. S. Acharya (Toyko: Universal Academy), 169
Gopalswamy, N., Yashiro, S., Michalek, G., et al. 2002, ApJL, 572, L103
Gosling, J. T. 1993, JGR, 98, 18937
Grechnev, V. V., Kiselev, V. I., Meshalkina, N. S., & Chertok, I. M. 2015, SoPh, 290, 2827
Guo, F., & Giacalone, J. 2010, ApJ, 715, 406
Kahler, S. W. 1992, ARA&A, 30, 113
Kahler, S. W. 1994, ApJ, 428, 837
Kahler, S. W. 2001, JGR, 106, 20947
Kahler, S. W. 2016, ApJ, 819, 105
Kahler, S. W., Hildner, E., & Van Hollebeke, M. A. I. 1978, SoPh, 57, 429
Kahler, S. W., Reames, D. V., & Sheeley, N. R., Jr. 2001, ApJ, 562, 558
Kahler, S. W., Sheeley, N. R., Jr., Howard, R. A., et al. 1984, JGR, 89, 9683
Kahler, S. W., & Vourlidas, A. 2013, ApJ, 769, 143
Kallenrode, M.-B., Cliver, E. W., & Wibberenz, G. 1992, ApJ, 391, 370
Klecker, B., Hovestadt, D., Scholer, M., et al. 1984, ApJ, 281, 458
Lario, D., Kwon, R.-Y., Vourlidas, A., et al. 2016, ApJ, 819, 72
Lin, R. P. 1970, SoPh, 12, 266
Luhn, A., Klecker, B., Hovestadt, D., & Moebius, E. 1987, ApJ, 317, 951
Mason, G. M., Cohen, C. M. S., Cummings, A. C., et al. 1999a, GeoRL, 26, 141
Mason, G. M., Gloeckler, G., & Hovestadt, D. 1984, ApJ, 280, 902
Mason, G. M., Mazur, J. E., & Dwyer, J. R. 1999b, ApJL, 525, L133
Mason, G. M., Reames, D. V., von Rosenvinge, T. T., Klecker, B., & Hovestadt, D. 1986, ApJ, 303, 849
Mazur, J. E., Mason, G. M., Looper, M. D., Leske, R. A., & Mewaldt, R. A 1999, GeoRL, 26, 173
McCracken, K. G., Moraal, H., & Shea, M. A. 2012, ApJ, 761, 101
McDonald, F. B., & Van Hollebeke, M. A. I. 1985, ApJL, 290, L67
Mewaldt, R. A., Cohen, C. M. S., Labrador, A. W., et al. 2005, JGR, 110, A09S18
Mewaldt, R. A., Looper, M. D., Cohen, C. M. S., et al. 2012, SSRv, 171, 97
Meyer, J.-P. 1985, ApJS, 57, 151
Miller, J. A., Cargill, P. J., Emslie, A. G., et al. 1997, JGR, 102, 14631
Müller-Mellin, R., Kunow, H., Fleißner, V., et al. 1995, SoPh, 162, 483
Nitta, N. V., Reames, D. V., De Rosa, M. L., et al. 2006, ApJ, 650, 438
Pesce-Rollins, M., Omodei, N., Petrosian, V., et al. 2015, arXiv:1507.04303
Ramaty, R., Murphy, R. J., & Dermer, C. D. 1987, ApJL, 316, L41
Reames, D. V. 1990, ApJS, 73, 235
Reames, D. V. 1993, AdSpR, 13, 331
Reames, D. V. 1999, SSRv, 90, 413
Reames, D. V. 2009a, ApJ, 693, 812
Reames, D. V. 2009b, ApJ, 706, 844
Reames, D. V. 2013, SSRv, 175, 53
Reames, D. V. 2015, SSRv, 194, 303
Reames, D. V. 2016, SoPh, 291, 911
Reames, D. V., Barbier, L. M., & Ng, C. K. 1996, ApJ, 466, 473
Reames, D. V., Cliver, E. W., & Kahler, S. W. 2014, SoPh, 289, 3817
Reames, D. V., Cliver, E. W., & Kahler, S. W. 2015, SoPh, 290, 1761
Reames, D. V., Meyer, J. P., & von Rosenvinge, T. T. 1994, ApJS, 90, 649
Reames, D. V., & Ng, C. K. 2004, ApJ, 610, 510
Reames, D. V., von Rosenvinge, T. T., & Lin, R. P. 1985, ApJ, 292, 716
Reinhard, R., & Wibberenz, G. 1974, SoPh, 36, 473
Richardson, I. G., von Rosenvinge, T. T., Cane, H. V., et al. 2014, SoPh, 289, 3059
Rouillard, A. P., Sheeley, N. R., Jr., Tylka, A., et al. 2012, ApJ, 752, 44
Ryan, J. M. 2000, SSRv, 93, 581
Ryan, J. M., & Lee, M. A. 1991, ApJ, 368, 316
Švestka, Z., & Fritzová-Švestková, L. 1974, SoPh, 36, 417
Thakur, N., Gopalswamy, N., Mäkelä, P., et al. 2016, SoPh, 291, 513
Trottet, G., Samwel, S., Klein, K.-L., Dudok de Wit, T., & Miteva, R. 2015, SoPh, 290, 819
Tylka, A. J., Cohen, C. M. S., Dietrich, W. F., et al. 2003, in Proc. 28th ICRC, ed. T. Kajita et al. (Tokyo: Universal Academy), 6, 3305
Tylka, A. J., Cohen, C. M. S., Dietrich, W. F., et al. 2005, ApJ, 625, 474
Tylka, A. J., & Lee, M. A. 2006, ApJ, 646, 1319
Vršnak, B., & Cliver, E. W. 2008, SoPh, 253, 215
Wild, J. P., Smerd, S. F., & Weiss, A. A. 1963, ARA&A, 1, 291